

# Molecular Dissociation in Presence of a Catalyst II: The bond breaking role of the transition from virtual to localized states.

A. Ruderman<sup>1,2</sup>, A. D. Dente<sup>3</sup>, E. Santos<sup>1,2</sup>, and H. M. Pastawski<sup>1</sup>

<sup>1</sup>*Instituto de Física Enrique Gaviola (CONICET), Facultad de Matemática, Astronomía y Física, Universidad Nacional de Córdoba, 5000, Córdoba, Argentina*

<sup>2</sup>*Institute of Theoretical Chemistry, Ulm University, D-89069, Ulm, Germany*

<sup>3</sup>*INVAP S.E., 8403, San Carlos de Bariloche, Argentina*

February 26, 2022

## Abstract

We address a molecular dissociation mechanism that is known to occur when a  $H_2$  molecule approaches a catalyst with its *molecular axis parallel to the surface*. It is found that molecular dissociation is a form of quantum dynamical phase transition associated to an analytic discontinuity of quite unusual nature: the molecule is destabilized by the transition from non-physical virtual states into actual localized states. Current description complements our recent results for a molecule approaching the catalyst with its *molecular axis perpendicular to the surface* [1]. Also, such a description can be seen as a further successful implementation of a non-Hermitian Hamiltonian in a well defined model.

## 1 Introduction

How do molecules form? This has been recognized as one of the ten unsolved mysteries of Chemistry, enumerated in 2013 for the Year of Chemistry

Celebration [2]. Indeed, a new entity emerges when two identical atoms meet. The reciprocal is also true: as a dimer approaches a catalyst’s surface, it may break down. But when and how does this break down precisely happen? What distinguishes these two different quantum objects, i.e. the molecule and the two independent atoms? It is natural to think that as some control parameter move, e.g. an inter-atomic distance, a sort of discontinuity or phase transition should happen. While a quantum calculation can be set up to simulate such reaction, the calculations of an increasingly realistic system quickly begin to overwhelm even the most powerful computer. While DFT calculations hint a change in chemical bonds as the molecule-catalyst interaction increases when the molecule approaches to the surface [3], this is confronted with the fact that in a finite system no actual discontinuities can happen. The key for the molecule formation/dissociation mystery can be found in P. W. Anderson’s inspiring paper “More is Different” [4]. There, Anderson recalled that the inversion oscillations in ammonia-like molecules suffer a sort of transition into a non-oscillating mode as the masses are increased. Much as in a classical oscillator transition to an over-damped regime, the crucial ingredient is the infinite nature of the environment which induces dissipation while preventing the occurrence of Poincare’s recurrences and enable a dynamical phase transition. These concepts were formalized in the context of the Rabi oscillations in a quantum system: a spin dimer immersed in an environment of spins. Since this is solved in the thermodynamic limit of infinitely many spins which provide the crucial continuum spectrum. [5, 6]. In this case, the finite Rabi frequency undergoes a non-analytic transition into a non-oscillatory mode as the interaction with the environment increases [7, 8, 9]. This mathematical discontinuity was termed Quantum Dynamical Phase Transition (QDPT) [10].

While the application of these ideas to molecular dissociation/formation is not completely straightforward, in a previous paper we succeeded in describing H<sub>2</sub> molecule formation/dissociation in the presence of a catalyst as a QDPT [1]. This description was achieved using a variant of the model introduced by D. M. Newns for hydrogen adsorption in a metallic surface [11]. However, that analysis was restricted to the case when *the molecular axis is perpendicular to the catalyst surface*. In [1] the environment provides the infinitely many catalyst orbitals whose influence had to be treated beyond linear response. Indeed, the interaction among the crystal states and the dimer orbitals dramatically perturb each other and has to be obtained through a self-consistent Dyson equation. In particular, the substrate induces imaginary corrections to the molecular energies, accounting for their finite lifetime. These complex energies, as those obtained from the Fermi Golden Rule, represent resonances and are accounted by a non-Hermitian Hamilto-

nian [12]. Our main result was that two *resonances are formed inside* the  $d$  band and that they present analytical discontinuities as a function of the molecule-substrate interaction (distance) [13, 14, 15]. Thus, the *molecular dissociation/formation* was identified as the non-analytic *collapse/splitting of these resonances*.

In this paper, we address another reaction mechanism that is known to occur when a  $\text{H}_2$  molecule approaches a catalyst with its *molecular axis parallel to the surface*. It is found that molecular dissociation is also a phase transition associated to an analytic discontinuity, but of different and unusual nature: the molecule is destabilized by the transition from non-physical virtual states into actual localized states. For the rest of the article we will be dealing with the same model and tools introduced in our previous work [1] which, in this case, provide substantially new perspective into the molecular dissociation/formation problem.

## 2 The model

Given a homonuclear molecule AB and a metal electrode with a half filled  $d$  band, two independent geometries arise to describe the interaction. The particular configuration of a molecule approaching with its axis perpendicular to the metal surface, was previously investigated in reference [1]. A fully different problem arises when the axis along the molecule lies parallel to the surface. In this configuration the distances between a given atom belonging to the metal surface and both atoms forming the molecule remain equal, i.e.  $d_A = d_B = d$  ( see Fig. 1). Therefore, both atoms interact identically with the metal, resulting in a completely different Hamiltonian respect to the perpendicular case, and hence yielding a dissimilar kind of transition.

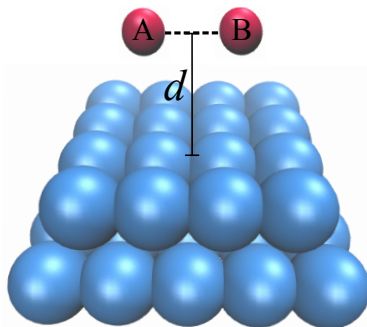


**Figure 1:** Homonuclear molecule interacting with a metallic surface. The principal axis of the molecule is parallel to the surface and the distance of each atom to the substrate are the same.

To set up the model Hamiltonian for the interaction between the molecule and the metal, we write the molecule's Hamiltonian as:

$$\hat{H}_{\text{mol}} = E_A |A\rangle \langle A| + E_B |B\rangle \langle B| - V_{AB} (|A\rangle \langle B| + |B\rangle \langle A|).$$

The atomic energies  $E_A$  and  $E_B$  are identical and their degeneracy is broken by the mixing element  $-V_{AB}$  that leads to the bonding and antibonding states, i.e. the Highest Occupied Molecular Orbital (HOMO) and Lowest Unoccupied Molecular Orbital (LUMO), respectively. In this orientation, the molecule only can have substantial overlap with the metal  $d_{z^2}$  and  $d_{xz}$  orbitals of the underlying metallic atom. Therefore,  $z$  is considered to be perpendicular to the surface and  $x$  is chosen parallel to the molecular axis. Both orbitals interact with the target molecule in different ways [16], as depicted in Fig. 2. On one side, the overlap of the  $d_{z^2}$  with the atomic orbitals A and B have the same the sign and magnitude, resulting in a Hamiltonian coupling element  $-V_0$ . On the other side, the molecule also interacts with the  $d_{xz}$  orbital of the metal. In this case, while having equal strengths a different sign appears for each atomic orbital. Taking these considerations into account, there are two concurrent mechanisms for molecule-metal interaction :

$$\hat{V}_{\text{int}} = V_0(|A\rangle \langle d_{z^2}| + |B\rangle \langle d_{z^2}|) + \lambda V_0(-|A\rangle \langle d_{xz}| + |B\rangle \langle d_{xz}|),$$

where  $|d_{z^2}\rangle$  and  $|d_{xz}\rangle$  are the metallic orbitals that interact with the molecule. Furthermore, we have included a  $\lambda$  factor to account for the difference among the interaction strengths with the two  $d$  orbitals.

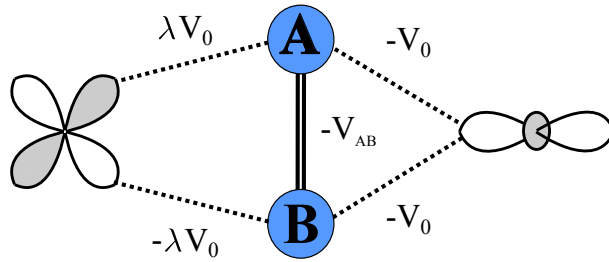


**Figure 2:** Different signs for the interaction between the molecule and the metallic atomic orbital, due to the lobe phase shift for the atomic orbital functions  $d_{z^2}$  and  $d_{xz}$ . The  $\lambda$  factor accounts for the different strength interaction between the molecule and the orbitals  $d_{z^2}$  and  $d_{xz}$ .

In Fig. 2 we represent explicitly two, assumed independent, sets of metallic  $d$  orbitals associated with each symmetry of the surface orbitals (i.e.  $|d_{z^2}\rangle$  and  $|d_{xz}\rangle$ ). Therefore, the relevant part of the metal Hamiltonian can be represented using a narrow band model. This approximation was first proposed by Newns [11], who stated that the projection of the  $d$  band Local

Density of States (LDoS) over the specific orbital (either  $d_{z^2}$  or  $d_{xz}$ ) could be schematized as a semielliptic energy band that strongly interacts with the molecule [17]. This picture is validated by appealing to a Lanczos’s transformation [1, 18, 19] to obtain this simple electronic structure for the  $d$  band. The basic procedure is visualised in Fig. 3 for a two dimensional metal represented as two distinct collections of orthonormal  $d$  orbitals. By choosing one of the interacting metallic orbitals as a reference, the intermetallic interactions provide (through the Lanczos’s procedure) for combination of atomic  $d$  orbitals consistent with the initial symmetry. Typically, these are progressively included according to their distance to the initial orbital. These “collective” substrate orbitals are naturally arranged in the Hilbert space in order to evidence the tridiagonal nature of the Hamiltonian in the new basis. By means of this procedure, the general three dimensional geometry of a catalyst is reduced to a effective linear chain. The same reasoning applies for both symmetries. Then, we can write the metal  $d_{z^2}$  Hamiltonian as:

$$\hat{H}_{\text{met}}^{z^2} = \sum_{n=1}^{\infty} E_n^{z^2} |n\rangle \langle n| - \sum_{n=1}^{\infty} V_{n,n+1}^{z^2} (|n\rangle \langle n+1| + |n+1\rangle \langle n|), \quad (1)$$

where  $|n\rangle$  and  $E_n^{z^2}$  are the  $n$ -th collective metal orbital obtained by the Lanczos’s transformation and the energy corresponding to that orbital, respectively. For the sake of simplicity, all the hopping elements  $V_{n,n+1}^{z^2}$  are considered to be equal to  $V$ . This is consistent with the fast convergence of the hopping elements, first addressed by Haydock et al. [19]. A similar Hamiltonian  $\hat{H}_{\text{met}}^{xz}$  is obtained for the  $xy$  symmetry. Thus,

$$\hat{H}_{\text{met}} = \hat{H}_{\text{met}}^{z^2} + \hat{H}_{\text{met}}^{xz}.$$

In order to obtain an optimal configuration for our discussion on the dissociation process [20], we make the  $d$  band to be centered around the Fermi energy  $E$  by making  $E_A = E_B = E_n = E$ . Then, the bonding and antibonding molecular states, i.e. HOMO and LUMO, fall outside the band as  $2|V_{AB}| > 4|V|$  [21]. This choice is consistent with the standard knowledge of the Marcus-Hush theory for optimal conditions of electron transfer and molecular dissociation. In this work, we used  $V_{AB}/V = 2.5$  which is typical for  $\text{H}_2$ .

The main features of the system, i.e. energy spectrum and relevant eigenvalues properties, could be obtained using a decimation procedure [22, 23]. This formulation deploys an infinite order perturbation theory for the interaction  $\hat{V}_{\text{int}}$  to dress the molecular Hamiltonian  $\hat{H}_{\text{mol}}$  into an effective molecular

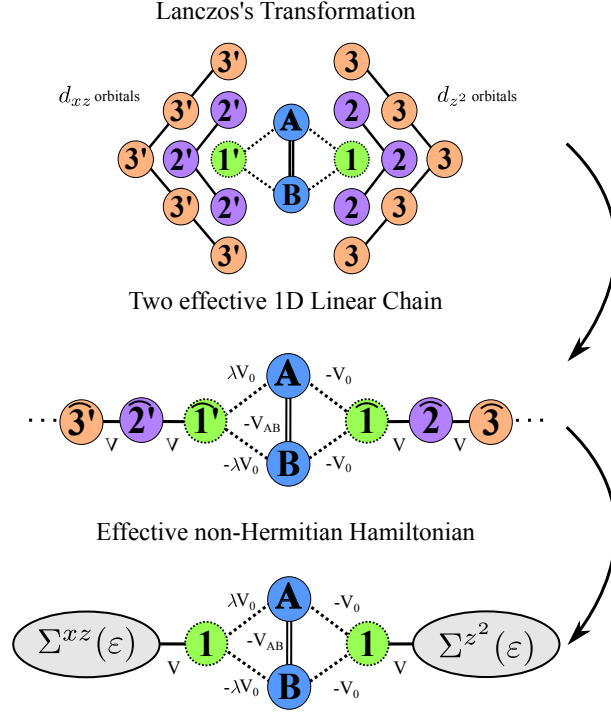


**Figure 3:** Effective non-Hermitian Hamiltonian due Lanczos's transformation from a molecule A-B (in blue), interacting with a 2D metal substrate composed of two distinct collections of  $d$  orbitals. The transformation implies combining each layer of orbitals at the same distance of the interacting atom. The decimation process results in a four dimensional Hamiltonian with the metal represented as two effective self-energies.

Hamiltonian that accounts for the presence of the catalyst, and yields a complex correction,  $\Sigma$ , to the molecular bonding and antibonding energies. This is sketched in the bottom panel of Fig. 3. This precisely defined procedure resorts to the Green's function matrix associated with the total Hamiltonian  $\hat{H} = \hat{H}_{\text{mol}} + \hat{H}_{\text{met}} + \hat{V}_{\text{int}}$ ,

$$\mathbb{G}(\varepsilon) = (\varepsilon\mathbb{I} - \mathbb{H})^{-1}. \quad (2)$$

We are going to profit from the fact that the poles of the Green's function are the eigenvalues of the system. At this point, a brief introduction to the decimation technique is convenient for the sake of clarity. Let us first consider the molecular Hamiltonian without the presence of the metal:

$$\mathbb{H}_{\text{mol}} = \begin{bmatrix} E_A & -V_{AB} \\ -V_{AB} & E_B \end{bmatrix}. \quad (3)$$

Then, the Green's function matrix adopts the form:

$$\mathbb{G}_{\text{mol}} = \frac{1}{(\varepsilon - E_A)(\varepsilon - E_B) - |V_{AB}|^2} \begin{bmatrix} \varepsilon - E_B & V_{AB} \\ V_{AB} & \varepsilon - E_A \end{bmatrix}. \quad (4)$$

The Green's function for atom A, the first diagonal element of  $\mathbb{G}_{\text{mol}}$ , can be written as

$$G_{\text{mol}}^{AA} = (\varepsilon - E_A - \Sigma_A)^{-1}$$

Therefore, the energy of atom A is modified by the presence of the atom B through the self-energy

$$\Sigma_A = |V_{AB}|^2 / (\varepsilon - E_B).$$

This decimation procedure can be extended to the full semi-infinite chain that describes the components of the  $d$  band that couple with the HOMO and LUMO according to their symmetry. The procedure consists on “dressing” the successive “Lanczos's orbitals” with the corresponding self-energies to account for the interaction with the neighbour atom at the right. In a finite system of  $N + 2$  orbitals,  $\Sigma_A$  is written in terms of  $N + 1$  levels of a continued fraction until one reaches the last level. To simplify the study of the spectral density, the energies of the system can be renormalized by introducing an imaginary small quantity  $-i\eta$ , thus  $E \rightarrow E - i\eta$ . This energy correction can be seen as a weak environmental interaction, a role that could be assigned to the  $sp$  band states [24]. Thus, in the thermodynamic limit of a semi-infinite chain ( $N \rightarrow \infty$ ), the self-energy correction due to the metal becomes:

$$\Sigma(\varepsilon) = \frac{|V|^2}{\varepsilon - (E - i\eta) - \Sigma(\varepsilon)} = \Delta(\varepsilon) - i\Gamma(\varepsilon), \quad (5)$$

By setting  $E = 0$  in the whole system (i.e. setting down the Fermi level as the energy reference) the analysis is further simplified. Equation 5 has two solutions with different signs. The solution with physical meaning provides a retarded response and results:

$$\Sigma(\varepsilon) = \frac{\varepsilon + i\eta}{2} - \text{sgn}(\varepsilon) \times \left( \sqrt{\frac{r+x}{2}} + i \times \text{sgn}(y) \times \sqrt{\frac{r-x}{2}} \right), \quad (6)$$

with  $x = \frac{\varepsilon^2 - \eta^2}{2} - V^2$ ,  $y = \frac{\varepsilon\eta}{2}$  and  $r = \sqrt{x^2 + y^2}$ .

Then, the restriction to the first four orbitals of the total Hamiltonian can be written in a simple way:

$$\tilde{\mathbb{H}} = \begin{bmatrix} \Sigma^{z^2}(\varepsilon) & -V_0 & -V_0 & 0 \\ -V_0 & -i\eta & -V_{AB} & +\lambda V_0 \\ -V_0 & -V_{AB} & -i\eta & -\lambda V_0 \\ 0 & +\lambda V_0 & -\lambda V_0 & \Sigma^{xz}(\varepsilon) \end{bmatrix}. \quad (7)$$

Now, a basis change can be made to a molecular *bonding* and *antibonding* representation. Equation 8 shows the Hamiltonian in the new basis. Notice that, the bonding state (second diagonal element) does not interact with  $\Sigma^{xz}(\varepsilon)$  (fourth diagonal element) and the antibonding state (third diagonal element) does not interact with  $\Sigma^{z^2}(\varepsilon)$  (first diagonal element):

$$\tilde{\mathbb{H}}' = \tilde{\mathbb{H}}_+ \otimes \tilde{\mathbb{H}}_- = \begin{bmatrix} \Sigma^{z^2}(\varepsilon) & -\sqrt{2}V_0 & 0 & 0 \\ -\sqrt{2}V_0 & -V_{AB} - i\eta & 0 & 0 \\ 0 & 0 & V_{AB} - i\eta & \sqrt{2}\lambda V_0 \\ 0 & 0 & \sqrt{2}\lambda V_0 & \Sigma^{xz}(\varepsilon) \end{bmatrix}. \quad (8)$$

Therefore, the system is naturally detached in two portions in which the Green's function matrices can be solved independently. For the bonding subspace, i.e. the bonding molecular orbital interacting with  $\Sigma^{z^2}(\varepsilon)$ , the Green's function takes the form:

$$\mathbb{G}_+ = \frac{1}{(\varepsilon + V_{AB} + i\eta)(\varepsilon - \Sigma^{z^2}(\varepsilon)) - 2V_0^2} \begin{bmatrix} \varepsilon + V_{AB} + i\eta & -\sqrt{2}V_0 \\ -\sqrt{2}V_0 & \varepsilon - \Sigma^{z^2}(\varepsilon) \end{bmatrix}, \quad (9)$$

while, for the antibonding molecular orbital interacting with  $\Sigma^{xz}(\varepsilon)$ , there is a subspace where

$$\mathbb{G}_- = \frac{1}{(\varepsilon - V_{AB} + i\eta)(\varepsilon - \Sigma^{xz}(\varepsilon)) - 2(\lambda V_0)^2} \begin{bmatrix} \varepsilon - \Sigma^{xz}(\varepsilon) & \sqrt{2}\lambda V_0 \\ \sqrt{2}\lambda V_0 & \varepsilon - V_{AB} + i\eta \end{bmatrix}. \quad (10)$$

For the rest of the article  $\lambda$  will be set  $\lambda \sim 1$  and  $\Sigma^{xz} = \Sigma^{z^2}$ . The eigenenergies and resonances of the system are obtained by finding the poles of Eqs. 8 and 9. This is achieved solving the equations:

$$\varepsilon + V_{AB} - 2\alpha\Sigma(\varepsilon) = 0, \quad (11)$$

$$\varepsilon - V_{AB} - 2\alpha\Sigma(\varepsilon) = 0. \quad (12)$$

Equation 11 accounts for the poles corresponding to the bonding state interacting with the  $d_{z^2}$  band and Eq. 12 for the poles of the antibonding state interacting with the  $d_{xz}$  band.

### 3 Molecular dissociation

A first hint for molecular dissociation arises from analysing the molecular bonding orbital that interacts with the  $d$  band through the  $d_{z^2}$  orbital, Fig.

4. In this case, Eq. 11 provides two poles which are below the  $d$  band at the molecular bonding energy  $\varepsilon = -V_{AB}$ . One is a physical localized pole (green line in Fig. 4) which corresponds to the bonding state  $|AB\rangle$ . As the interaction increases,  $|AB\rangle$  evolves to a bonding combination between the bonding state of the molecule and the metal, i.e.  $|((AB)d_{z^2})\rangle$ , becoming more localized and its energy lying well below the Fermi level. The other pole corresponds to a non-physical virtual state which, as the interaction increases, escapes to negative energies and reappears at positive values (red dots in Fig. 4). As the non-physical pole gets closer to the  $d$  band, it finally meets the band-edge and suffers a transition into a physical localized state. This is an antibonding combination between the molecular bonding state and the metal  $|((AB)d_{z^2})^*\rangle$  (blue line). In this scenario, bond weakening occurs because occupying the  $|((AB)d_{z^2})\rangle$  state implies diminishing the occupation of the bonding  $|AB\rangle$  from 100% into a final 50%. Indeed, the molecular bonding state now has 50% participation in the unoccupied  $|((AB)d_{z^2})^*\rangle$  localized orbital that emerged from the upper top of the  $d$  band.

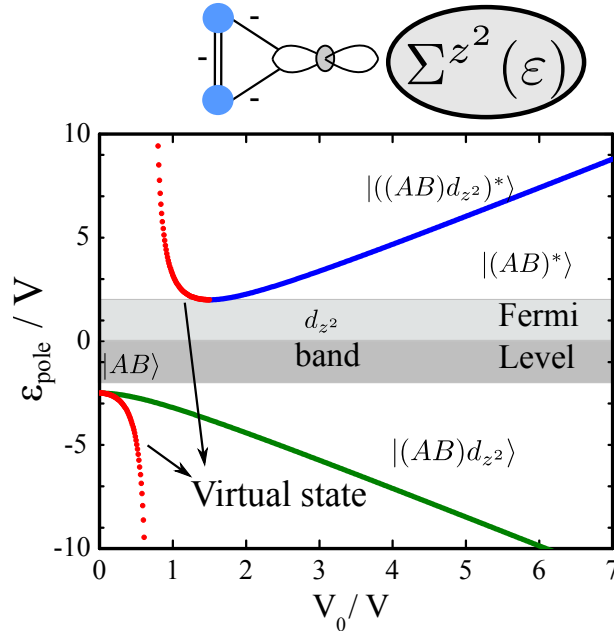


**Figure 4:** Poles of the Green's function for the parallel configuration when the molecule interacts with the  $d_{z^2}$  orbital.

The previous discussion has a precise equivalence in the analysis of the states that evolve from the molecular antibonding state. However, the same formulation has now completely different meaning. The molecular antibonding state interacts with the  $d$  band through  $d_{xz}$ . The poles resulting from

Eq. 12, are shown in Fig. 5. At the antibonding energy  $\varepsilon = V_{AB}$ , two poles appear. A physical localized state, related to the molecular antibonding state  $|((AB)^*)\rangle$  (blue line in Fig. 5), whose energy increases as  $V_0$  increases and becomes an antibonding combination between the molecular antibonding state and the metal site  $|((AB)^*d_{xz})^*\rangle$ . The other pole at  $\varepsilon = V_{AB}$  is a virtual state [25, 26] (red dots in Fig. 5) which diverges as  $V_0$  increases and appears again from  $-\infty$  until its energy touches the  $d$  band. At this critical value, the virtual state suffers a transition and becomes a localized state (green line in Fig. 5) which is a bonding combination between the molecular antibonding state and the metal band  $|((AB)^*d_{xz})\rangle$ . Therefore, molecular dissociation can be interpreted as occurring at the precise value when the virtual pole touches the  $d$  band and becomes the localized, and occupied, state  $|((AB)^*d_{xz})\rangle$ . Thus, molecular dissociation occurs at a non-analytical point of the physical observables, e.g. total energies. At this point the molecular electrons have a transition from an increasingly occupied bonding state that participates of the delocalized band into a localized combination between the  $d$  states and antibonding molecular orbital. This is a form of Quantum Dynamical Phase Transition which, to the best of our knowledge, has not been identified before in the context of molecular dissociation.

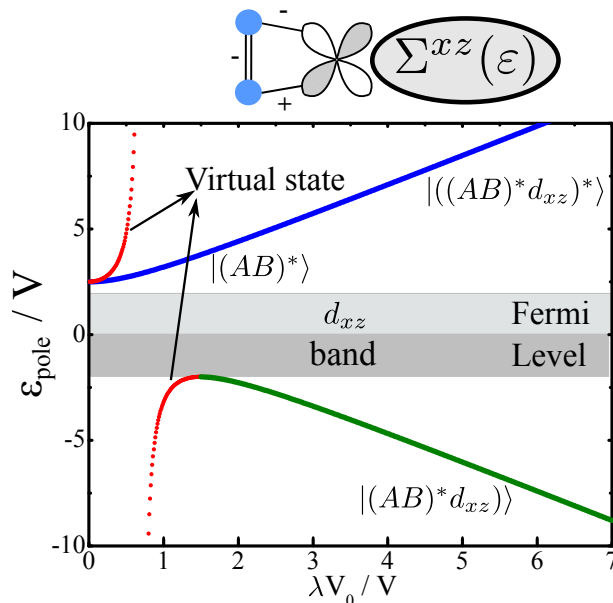


**Figure 5:** Poles of the Green's function for the parallel configuration when the molecule interacts with the  $d_{xz}$  orbital. The molecule dissociation as a QDPT can be observed when the interaction is with the  $d_{xz}$  band.

From the results it becomes evident that the most interesting situation is

when the antibonding molecular orbital interacts with the  $d_{xz}$ . From Eq. 10 we get the diagonal Green's function at the  $d_{xz}$  metallic orbital:

$$G_{d_{xz}}(\varepsilon) = \frac{1}{\varepsilon + i\eta - \Sigma(\varepsilon) - \frac{2(\lambda V_0)^2}{\varepsilon + i\eta + V_{AB}}}. \quad (13)$$

The LDoS for the  $d$  band can be obtained from Eq. 13,

$$N_{d_{xz}}(\varepsilon) = -\frac{1}{\pi} \lim_{\eta \rightarrow 0^+} \text{Im} [G_{d_{xz}}(\varepsilon)], \quad (14)$$

which becomes of great help to reinforce and extend the previous discussion. This LDoS is shown in Fig. 6 for  $\lambda V_0/V$  between 0 and 3.6 for  $\lambda = 1$ . When  $V_0 \sim 0$  the shape of the LDoS corresponds to a non interacting  $d_{xz}$  band. As  $\lambda V_0$  increases the  $d_{xz}$  band starts to mix with the antibonding state of the dimer. The energy of this antibonding combination  $|((AB)^*d_{xz})^*\rangle$ , progresses toward increasingly positive values as the interaction grows. Meanwhile, the virtual state approaches the  $d_{xz}$  band from negative energies while it produces an ‘‘attraction’’ that increases the LDoS near the band edge. As the virtual state meets the band a localized state *emerges* from the band edge and gains weight. A similar issue was recently discussed in the context of engineered plasmonic excitations in metallic nanoparticle arrays [26]. There, it was shown analytically that the distorted band is the product among the original semi-elliptic band and a Lorentzian centered in the virtual state. This concentrates a density of states near band edge until it becomes a divergence and a localized state is expelled at a critical interaction strength, shown as a dot in Fig. 5.

The previous conclusion is reinforced by the analysis of LDoS at the antibonding orbital. Figure 7 shows how the unoccupied antibonding state  $|((AB)^*)\rangle$  loses its weight towards a participation on combination with the  $d_{xz}$  band which finally emerges as an *occupied localized state*. This is a crucial contribution to molecular destabilization. As in the first part of this work [1] the new transition can be seen as a successful implementation of a non-Hermitian Hamiltonian [12] in a well defined model.

Notice that Figs. 6 and 7 also serve to discuss the interaction between the bonding molecular state  $|AB\rangle$  and the  $d_{z^2}$  band by exchanging the sign of the energy. Thus, in this case, the  $|((AB)d_{z^2})^*\rangle$  emerges as an unoccupied localized state above the  $d_{z^2}$  band, while  $|AB\rangle$  state loses occupation as the  $|((AB)d_{z^2})\rangle$  state forms with increasing interaction.

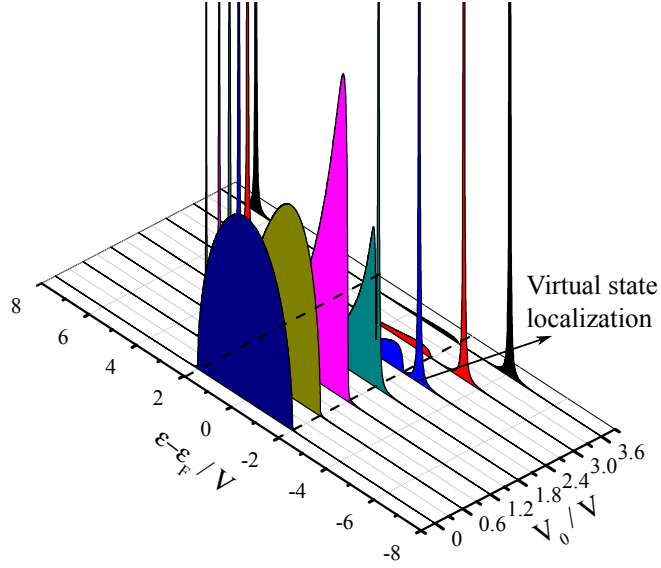


**Figure 6:** LDoS of the  $d$  band. As  $V_0$  increases a state is expelled from the band and, after the transition point, forms the localized state  $| (AB)^* d_{xz} \rangle$ ,  $\eta = 0.01$  eV.

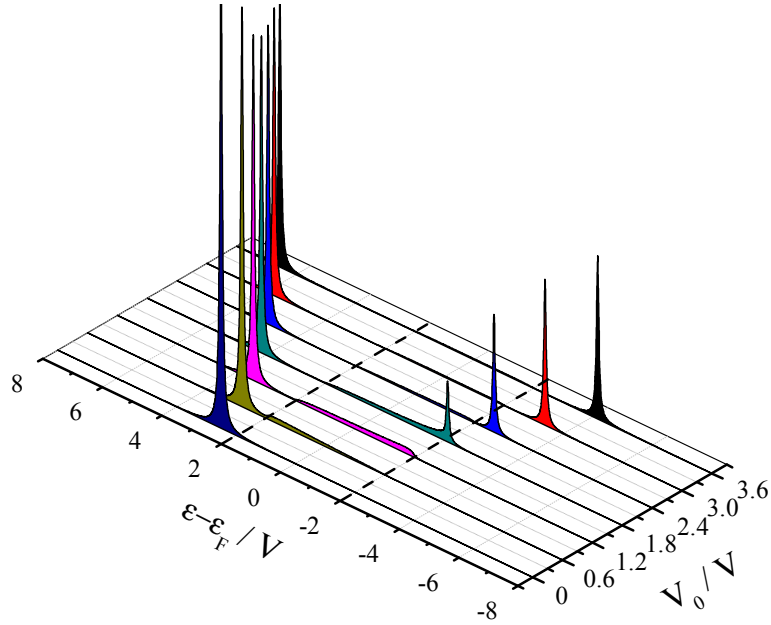


**Figure 7:** LDoS of the molecular antibonding state  $| (AB)^* \rangle$ , interacting with the metallic orbital  $d_{xz}$ , as  $V_0$  increases,  $\eta = 0.05$  eV.

## 4 Conclusions

As a  $\text{H}_2$  molecule approaches a catalyst with its axis parallel to the surface, the interaction creates two independent collective orbitals which are superpositions with different surface  $d$  orbitals that are part of their corresponding metallic bands. The molecular bonding state becomes mixed with the  $d_{z^2}$  band while the molecular antibonding state interacts with the  $d_{xz}$  band. This gives rise to two processes described by the same algebra, but with different physical meanings as their energies are the reverse of each other.

On one side, the mixing of the molecular bonding state produces a decrease of its occupation. While this occurs, the LDoS of the  $d_{z^2}$  band is distorted at its upper edge much as if it were “attracted” upwards. Finally, at a critical interaction strength the divergent peak is expelled as a localized state emerging from the upper (i.e. unoccupied) part of the  $d_{z^2}$  band. This new *unoccupied* state is an antibonding combination among the surface  $d_{z^2}$  orbital and the *bonding* state of the dimer.

On the other side, a fraction of the molecular antibonding state gets increasingly mixed with the  $d_{xz}$  metallic band. This produces a decrease of the dimer participation on its unoccupied antibonding combination. Simultaneously, the  $d_{xz}$  LDoS is “attracted” towards its lower edge until it finally emerges as an *occupied localized state* build as a bonding combination among the molecular *antibonding* state and the  $d_{xz}$  band.

These simultaneous mixing processes, i.e. the depopulation of the molecular bonding state and the occupation of the molecular antibonding state, both schematized in Fig. 8, are responsible for the dimer destabilization that leads to its breakdown.

While the essence of the molecule dissociation mechanisms are already hinted by the resolution of toy models for the catalyst such as small metallic clusters or even a single metal atom, the criticality of the dissociation transition would not be readily captured. Indeed, as in the first part of this work [1], the quasi-continuum nature of a metallic substrate is crucial to describe dissociation as an analytical discontinuity. In this case, we interpreted dissociation as the emergence of the localized state from the band edges as the interaction strength increases. This is an actual quantum dynamical phase transition. Remarkably, the elusive virtual states (i.e. states that are non-physical poles of  $\mathbb{G}(\varepsilon)$  [27, 28]) acquire a physical meaning as “attractors” of a distortion of the continuum band creating a LDoS divergence that finally expels a localized state. This is, a non-analytical transition.

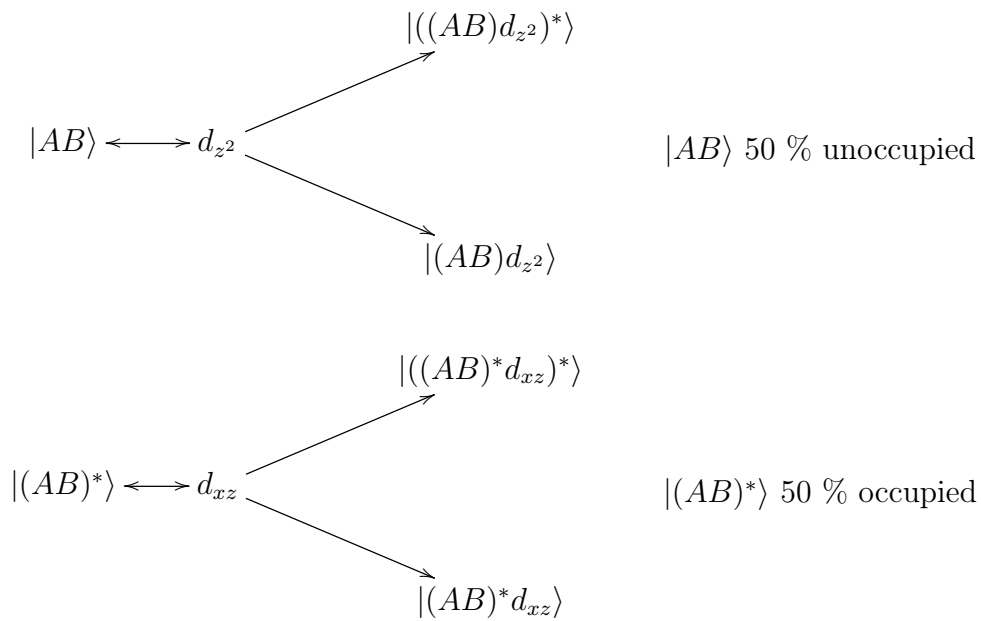


**Figure 8:** The interaction of the bonding molecular orbital with the  $d_{z^2}$  band shields an antibonding combination that depopulates this molecular orbital, while the occupied fraction loses weight towards the  $d_{z^2}$  band. Simultaneously, the interaction of the antibonding molecular orbital with  $d_{xz}$  band enforces this molecular state to split among an antibonding combination and an emergent bonding one that is interpreted as the molecular breakdown.

## Acknowledgements

We acknowledge the financial support from CONICET (PIP 112-201001-00411), SeCyT-UNC, ANPCyT (PICT-2012-2324) and DFG (research network FOR1376). We thank P. Serra and W. Schmickler for discussions and references.

## References

- [1] Ruderman, A.; Dente, A. D.; Santos, E.; Pastawski, H. M. *Journal of Physics: Condensed Matter* **2015**, *27*(31), 315501.
- [2] Ball, P. *Scientific American* **2011**, pages 48–53.
- [3] Santos, E.; Hindelang, P.; Quaino, P.; Schmickler, W. *Phys. Chem. Chem. Phys.* **2011**, *13*(15), 6992–7000.
- [4] Anderson, P. W. *Science* **1972**, *177*(4047), 393–396.
- [5] W. Anderson, P. *Journal of the Physical Society of Japan* **1954**, *9*(3), 316–339.
- [6] Álvarez, G. A.; Danieli, E. P.; Levstein, P. R.; Pastawski, H. M. *The Journal of Chemical Physics* **2006**, *124*(19).
- [7] Sachdev, S. *Quantum phase transitions*; Wiley Online Library, 2007.
- [8] Chibbaro, S.; Rondoni, L.; Vulpani, A. *Reductionism, emergence and levels of reality.*; Springer, 2014.
- [9] Leggett, A. J.; Chakravarty, S.; Dorsey, A.; Fisher, M. P.; Garg, A.; Zwerger, W. *Reviews of Modern Physics* **1987**, *59*(1), 1.
- [10] Pastawski, H. M. *Physica B: Condensed Matter* **2007**, *398*(2), 278–286.
- [11] Newns, D. M. Feb **1969**, *178*, 1123–1135.
- [12] Rotter, I.; Bird, J. *Reports on Progress in Physics* **2015**, *78*(11), 114001.
- [13] Berry, M. B. *Czech. J. of Phys* **2004**, *54*, 1039–1047.
- [14] Rotter, I. *J. Phys. A: Mathematical and Theoretical* **2009**, *42*(15), 153001.
- [15] Eleuch, H.; Rotter, I. *arXiv:1409.1149v1*.
- [16] Hoffmann, R. Jul **1988**, *60*, 601–628.
- [17] Xin, H.; Vojvodic, A.; Voss, J.; Nørskov, J. K.; Abild-Pedersen, F. *Physical Review B* **2014**, *89*(11), 115114.
- [18] Lanczos, C. *An iteration method for the solution of the eigenvalue problem of linear differential and integral operators*; United States Governm. Press Office, 1950.

- [19] Haydock, R.; Heine, V.; Kelly, M. J. *Journal of Physics C: Solid State Physics* **1972**, 5(20), 2845.
- [20] Hush, N. S. *The Journal of Chemical Physics* **1958**, 28(5).
- [21] Santos, E.; Bartenschlager, S.; Schmickler, W. *Journal of Electroanalytical Chemistry* **2011**, 660(2), 314–319.
- [22] Levstein, P. R.; Pastawski, H. M.; D’Amato, J. L. *Journal of Physics: Condensed Matter* **1990**, 2(7), 1781.
- [23] Pastawski, H. M.; Medina, E. *Rev. Mex. Fis.* **2001**, 47(1).
- [24] Cattena, C. J.; Bustos-Marín, R. A.; Pastawski, H. M. *Phys. Rev. B* **2010**, 82, 144201.
- [25] Dente, A. D.; Bustos-Marín, R. A.; Pastawski, H. M. *Phys. Rev. A* **2008**, 78, 062116.
- [26] Bustos-Marín, R. A.; Coronado, E. A.; Pastawski, H. M. *Physical Review B* **2010**, 82(3), 035434.
- [27] Landau, L. D.; Lifshitz, E. *Course of Theoretical Physics: Vol.: 3: Quantum Mechanis: Non-Relativistic Theory*; Pergamon Press, 1965.
- [28] Moiseyev, N. *Non-Hermitian Quantum Mechanics*; Cambridge Univ. Press., 2011.